Eur. Phys. J. B **60**, 325–336 (2007)
DOI: 10.1140/epjb/e2007-00358-1

THE EUROPEAN PHYSICAL JOURNAL B

Hydrodynamics of a rotating torus

R.M. Thaokar[1,a], H. Schiessel[2], and I.M. Kulic[3]

[1] Department of chemical engineering, Indian Institute of Technology, Bombay, Mumbai 400076, India
[2] Instituut-Lorentz, Universiteit Leiden, Leiden, Postbus, 9506, 2300 RA, The Netherlands
[3] School of Engineering and Applied Sciences, Harvard University, Cambridge, MA 02138, USA

Received 23 July 2007 / Received in final form 2 November 2007
Published online 22 December 2007 –

Abstract. The hydrodynamics of a torus is important on two counts: firstly, most stiff or semiflexible ring polymers, e.g. DNA miniplasmids are modeled as a torus and secondly, it has the simplest geometry which can describe self propelled organisms (particles). In the present work, the hydrodynamics of a torus rotating about its centerline is studied. Analytical expression for the velocity of a force free rotating torus is derived. It is found that a rotating torus translates with a velocity which is proportional to its internal velocity and to the square of the slenderness ratio, ϵ, similar to most low Reynolds number swimmers. The motion of a torus along a cylindrical track is studied numerically and it is observed that a force free torus changes its direction of motion (from a propelled state (weak wall effects) to a rolling state (strong wall effects)) as the diameter of the inner circular cylinder is increased. The rolling velocity is found to depend only on ϵ when the inner cylinder diameter approaches that of the torus.

PACS. 47.85.Dh Hydrodynamics, hydraulics, hydrostatics

1 Introduction

The list of models suggested to explain swimming at low Reynolds number is ever increasing, now spanning almost five decades [1–6]. The peculiarity of low Reynolds number flow lies in its quasi-static, time reversible nature, which renders impossible any reciprocal motion to propel the organism. This means that only certain types of shape changes that are non-reciprocal and break the time-reversal symmetry can make the microorganism move, and most suggested models in the literature take this into account [4–6]. Purcell [3] in his famous article on life at low Reynolds number, suggests a rotating torus which can translate as a possible mechanism of motility of living organisms. Similar recommendation was discussed by Taylor [7], although no calculations to date exist on the propulsion velocity of such an object and its dependence on the angular velocity about the centerline.

The other instance where a torus is encountered is the description of stiff and semiflexible polymer rings (e.g. DNA miniplasmids), which can be best modeled as a torus. Recently, we [8] proposed a nanomachine, consisting of a DNA mini-plasmid, which is set into rotations by rectifying thermal fluctuations, using the ratchet effect. In an extensive work on the hydrodynamics of a torus, Johnson [9] studied the flow around a torus for five different situations: Translation along the longitudinal axis, translation along the two transverse axes, rotation along the longitudinal axis (a spinning torus), on edge rotation and flow around an expanding torus. However, they did not address the problem of rotation around the centerline (Fig. 1a). There are very few studies that discuss this problem [10], although the self-propelled characteristics are not addressed in any of these and this forms the basis of the present study.

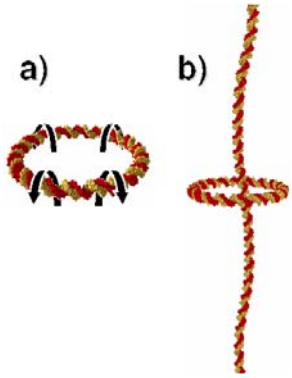

Fig. 1. Hydrodynamics of a torus: (depicted hereas a miniplasmid) (a) Translation of a single torus, (b) A torus moving along a cylindrical rail.

Interestingly, while suggesting a torus as a possible geometry to explain a low Reynolds number swimmer, Taylor [7] qualitatively argues about a situation in which a cylindrical rod threads through the hole in the torus (Fig. 1b). Such a torus would reverse its direction and

[a] e-mail: rochish@che.iitb.ac.in

can possibly go from a propulsion state to a rolling kind motion. In our recent work on a DNA miniplasmid as a nanomachine, we [8] argue that although a DNA miniplasmid can self-propel itself, its effect can be nullified by the substantial out of plane rotational diffusion prevalent in these machines owing to their small sizes [11]. This can be prevented though, by putting the DNA mini-plasmid on a rail, for example a DNA threading through the centerline. This is identical to a torus rotating about its centerline and moving along an infinitely long cylinder. Analytical solutions were obtained for the case of a slender torus moving inside a tube and the force acting on such a torus [12,13]. However, there are no calculations to date which address the motion of a rotating torus along a circular cylinder, and a possible reversal of direction, which is exactly the proposed mechanism for the nanomachine discussed by us [8].

In the present work, the hydrodynamics of a torus, rotating about its center-line in the zero Reynolds number limit is addressed, which is the relevant flow regime for less than micron sized objects. We construct the solution to this problem to an order higher in slenderness ratio ($O(b/a)^2$), than that considered earlier in the literature ($O(b/a)$), [10]. The full velocity profile for a rotating torus which is not allowed to translate is derived next and the force on such a torus is determined. Analytical results are presented in the limit of a slender torus, a limit which is relevant in for e.g. DNA mini-plasmids [8]. Although slender torus results are useful, especially in the case of polymer rings, there might be instances in which the torus thickness is of the same order as the internal radius, and the the boundary integral method is used to numerically solve the Stokes equation. We verify our analytical results using the numerical scheme and then extend the calculations to the non-slender limit. The problem of a force free torus moving along a cylindrical rod is addressed next. The force free velocity is calculated in several regimes and comparisons made with existing literature. The calculations are then extended to the lubrication limit.

2 Analytical solution of a rotating torus

Consider a torus with smaller diameter b and larger diameter a, rotating about its centerline with an angular velocity ω in a Newtonian fluid, in the zero Reynolds number limit (Fig. 2). In the analysis to follow, we indicate dimensional quantities by a tilde. The governing equations for the fluid are the Navier Stokes equations (continuity and momentum),

$$\tilde{\nabla} \cdot \tilde{\mathbf{u}} = 0 \tag{1}$$

$$\rho_f \left[\partial_{\tilde{t}} \tilde{\mathbf{u}} + \tilde{\mathbf{u}} \cdot \tilde{\nabla} \tilde{\mathbf{u}} \right] = -\tilde{\nabla} \tilde{p} + \mu \tilde{\nabla}^2 \tilde{\mathbf{u}} \tag{2}$$

where μ is the viscosity of the fluid. The physical quantities are non-dimensionalized as follows: The lengths are scaled by a, velocity with ωa, time by $1/\omega$, the stresses and the pressure by $\mu\omega$. With this non-dimensionalization the

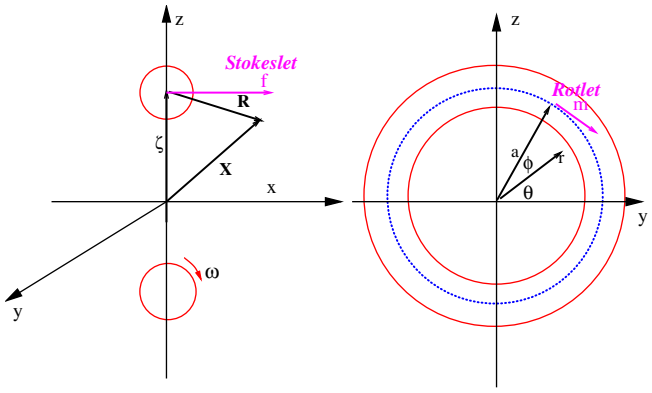

Fig. 2. Coordinate system for the torus: Local representation in cylindrical coordinates.

Navier Stokes equations are given by

$$\nabla \cdot \mathbf{u} = 0 \tag{3}$$

$$Re\,[\partial_t \mathbf{u} + \mathbf{u} \cdot \nabla \mathbf{u}\,] = -\nabla p + \nabla^2 \mathbf{u}, \tag{4}$$

where the Reynolds number $Re = a^2 \rho_f / (\mu\omega)$. For micron sized particles with speeds of few microns per second, the Reynolds number is indeed very low. In this work, we consider the limit of low Reynolds number, so that the Navier Stokes equations reduce to the familiar Stokes equations

$$\nabla \cdot \mathbf{u} = 0 \tag{5}$$

$$-\nabla p + \nabla^2 \mathbf{u} = 0. \tag{6}$$

Here we use two coordinate systems (Fig. 2), the Cartesian $(\mathbf{e_x}, \mathbf{e_y}, \mathbf{e_z})$, and the cylindrical coordinate system $(\mathbf{e_x}, \mathbf{e_r}, \mathbf{e}_\theta)$. The unit vectors of the two coordinate systems are related by

$$\mathbf{e_y} = \mathbf{e_r} \cos\theta + \mathbf{e}_\theta \sin\theta \tag{7}$$

$$\mathbf{e_z} = \mathbf{e_r} \sin\theta - \mathbf{e}_\theta \cos\theta. \tag{8}$$

The solution for velocity can be expressed in terms of fundamental solutions of Stokes flow like the rotlet, the Stokeslet, the stresslet and the potential dipole [15,16]. For a rotating torus about its centerline, we assume a uniform distribution of rotlets of strength $m\mathbf{e_x} \times \mathbf{e_r}$ acting along the center line of the torus, m is a scalar and $\mathbf{e_x}$ is the unit vector in the direction of the axis of symmetry of the torus. $\mathbf{e_r}$ is the unit vector joining the center line with any point on the surface of torus and $\mathbf{e_x} \times \mathbf{e_r}$ is tangent to the circle at point $\zeta = a\mathbf{e_r}$ [10]. The dominant singularity representing the velocity field of a "self propelled rotating torus" is expected to be the rotlet. The effect of the Stokeslet (force singularity) and the potential dipole (a higher order singularity) is considered later. The velocity in terms of the rotlet is then given by

$$\mathbf{u} = m \frac{(\mathbf{e_x} \times \zeta) \times \mathbf{R}}{R^3}. \tag{9}$$

Any reference point in the fluid, can be represented in cartesian coordinates (denoted with $()^c$) by

$\mathbf{X} = (x, r\cos\theta, r\sin\theta)^c$, while the centerline of the torus is given by $\tilde{\zeta} = (0, a\cos\phi, a\sin\phi)^c$. Here, θ is the azimuthal angle in the cylindrical coordinate system for any reference point X in the fluid, while ϕ defines the azimuthal angle subtended by the point rotlet ζ, acting along the centerline. Choosing the unit-length a, the vector joining the reference point and the centerline becomes $\mathbf{R} = \mathbf{X} - \zeta = (x, \sqrt{r^2+1-2r\cos(\phi-\theta)}, \phi-\theta)^{cyl}$ with $(...)^{cyl}$ denoting the cylindrical coordinates with magnitude R given by $\sqrt{r^2+x^2+1-2rcos(\phi-\theta)}$. The velocity at point $\mathbf{X}$ generated by the distribution of the point rotlets acting along the centerline can be obtained by integrating over ϕ. The velocity components are

$$u_x = \int_0^{2\pi} d\phi \left[m\frac{a - r\cos(\phi-\theta)}{R^3} \right] \tag{10}$$

$$u_r = \int_0^{2\pi} d\phi \left[mx\frac{\cos(\phi-\theta)}{R^3} \right] \tag{11}$$

$$u_\theta = \int_0^{2\pi} d\phi \left[mx\frac{\sin(\phi-\theta)}{R^3} \right]. \tag{12}$$

Since the rotlet is a special case of the fundamental solution which is identically annihilated by the Laplacian $\nabla^2\mathbf{u} = 0$, the pressure due to the rotlet, equation (6), is a constant. The flow due to a rotlet is vorticity free and it turns out to be a solution to both the Stokes and potential flow equations. This explains the similarity of results obtained in our work with the propulsion of vortex rings [17,18].

The angular component of the velocity goes to zero by symmetry. The velocities in equations (10) and (11) can be integrated and easily expressed in terms of complete elliptic integrals $E(k)$ and $K(k)$ (Appendix A), where k is defined as, $k^2 = 4r/\left[x^2+(r+1)^2\right]$.

The velocities in terms of these elliptic functions are given by (Appendix A),

$$u_x = \frac{m(I_3 - rI_4)}{C^3} \tag{13}$$
$$u_r = \frac{mxI_4}{C^3}$$

with $C = \sqrt{x^2+(r+1)^2}$ and I_3 and I_4 elliptic integrals given in Appendix A. The latter is exactly the result of [10].

In our analysis we consider external forces acting on the torus, and analyze two additional singularities, the potential dipole of strength d_{px} and the Stokeslet of strength f_x in the x direction. We now discuss the velocity due to a ring of point forces and point dipoles, distributed along the centerline. Consider the velocity due to a Stokeslet of strength f which is given by

$$\mathbf{u} = \left(\frac{\mathbf{I}}{R} + \frac{\mathbf{RR}}{R^3} \right) \cdot \mathbf{f}. \tag{14}$$

Here $\mathbf{RR}$ denotes the dyadic product, $\mathbf{I}$ is the identity matrix and $\mathbf{f}$ is a point force vector. The pressure due to a Stokeslet is given by

$$p = \frac{2\mathbf{R}\cdot\mathbf{f}}{R^3}. \tag{15}$$

An axially symmetric situation is considered here, i.e. a Stokeslet acting in the flow direction, x, and of constant magnitude f so that $\mathbf{f} = f_x\mathbf{e_x}$. The velocity is then given by

$$\mathbf{u} = \left(\frac{\mathbf{e_x}}{R} + \frac{\mathbf{R}x}{R^3} \right) f_x. \tag{16}$$

Similarly as in the rotlet case , using $\mathbf{R} = \mathbf{X} - \zeta$ with magnitude $R = \sqrt{x^2+(r+1)^2 - 4r\cos^2(\phi/2)}$, and integrating over the ϕ distribution of the ring of point Stokeslets, we obtain

$$u_x = f\int_0^{2\pi} d\phi \left[\frac{1}{R} + \frac{x^2}{R^3} \right] = f_x \left(\frac{I_1}{C} + x^2\frac{I_3}{C^3} \right) \tag{17}$$

$$u_r = fx\int_0^{2\pi} d\phi \left[\frac{r}{R^3} - \frac{\cos(\phi-\theta)}{R^3} \right] = \frac{xf_x(rI_3 - I_4)}{C^3} \tag{18}$$

$$p = 2fx\int_0^{2\pi} d\phi \left[\frac{\cos(\phi-\theta)}{R^3} \right] = \frac{2xf_xI_3}{C^3}. \tag{19}$$

It is known that the Stokeslet and its higher derivatives are solutions to Stokes equations [16]. Thus if $\mathbf{G}$ represents a Stokeslet then $\boldsymbol{\nabla^2\mathbf{G}}$ is also a solution to the Stokes equation and is called as the potential dipole. The velocity due to a potential dipole can be easily derived as

$$\mathbf{u} = \left(\frac{\mathbf{I}}{R^3} - \frac{\mathbf{3RR}}{R^5} \right) \cdot \mathbf{d}. \tag{20}$$

Consider the distribution of potential dipoles along a ring, acting in the x direction, such that $\mathbf{d} = d_{px}\mathbf{e_x}$, the x and the r directional velocities are given by,

$$u_x = d_{px}\int_0^{2\pi} d\phi \left[\frac{1}{R^3} - \frac{3x^2}{R^5} \right] = f_x \left(\frac{I_3}{C^3} - \frac{3x^2I_6}{C^5} \right) \tag{21}$$

$$u_r = 3xd_{px}\int_0^{2\pi} d\phi \left[-\frac{r}{R^5} + \frac{\cos(\phi-\theta)}{R^5} \right] = -\frac{3d_{px}x(rI_6 - aI_7)}{C^5}. \tag{22}$$

Note that there is no pressure contribution of the potential dipole [16]. The net velocity resulting from the contribution of the rotlets, Stokeslets and potential dipoles can be written as

$$u_x = \frac{m}{C^3}(I_3 - rI_4) + d_{px}\left(\frac{I_3}{C^3} - 3x^2\frac{I_6}{C^5} \right) + f_x\left(\frac{I_1}{C} + x^2\frac{I_3}{C^3} \right) \tag{23}$$

$$u_r = \frac{mxI_4}{C^3} - \frac{3d_{px}x}{C^5}(rI_6 - I_7) + \frac{xf_x}{C^3}(rI_3 - I_4)$$

$$p = \frac{2f_xxI_3}{C^3} \tag{24}$$

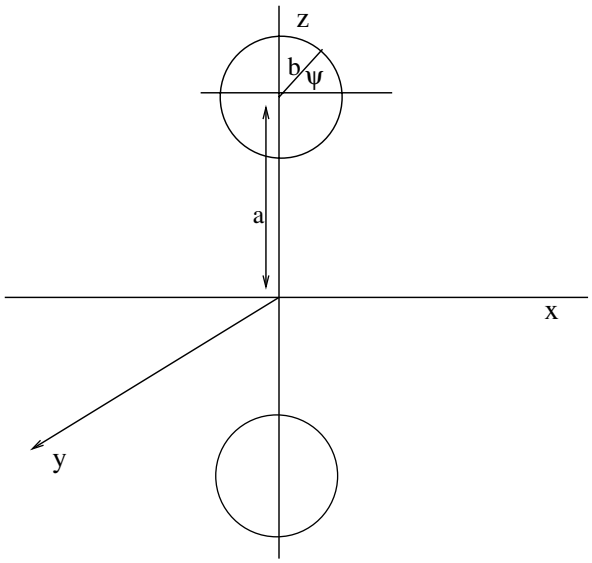

Fig. 3. Local parameterization of the torus.

where p is the pressure and has contribution only from the Stokeslet. For a torus rotating with angular velocity ω and translating with velocity U_x the boundary conditions are $\tilde{u}_x = \omega(a - \tilde{r}) + \tilde{U}_x$ and $\tilde{u}_r = \omega\tilde{x}$ at the surface of the torus. The non-dimensional boundary conditions thus become $u_x = (1 - r) + U_x$ and $u_r = x$. In the special case of an immobile torus, we set $U_x = 0$. We further consider here the case of a slender torus (the ratio of the two radii of the torus, $\epsilon = b/a$ is small), and the surface is locally parameterized by an angle ψ, such that $x = \epsilon\cos\psi$ and $r = 1 + \epsilon\sin\psi$ (Fig. 3). This implies the expansion $k^2 = 1 - \frac{\epsilon^2}{4} + O(\epsilon^3)$ in the slender torus limit. The asymptotic expressions for the elliptic integrals in the $k = 1$ limit (Appendix A) can therefore be used to simplify the expressions. The boundary conditions demand a scaling , $m = m_0\,\epsilon^2$, $d_{px} = \epsilon^4 d_{px0}$ and $f_x = \epsilon^2 f_{x0}$. The boundary conditions for the x and r directional no slip velocity conditions read as follows:

$$U_x - \epsilon\sin\psi = -2\epsilon m_o\sin\psi - \frac{\epsilon^2(m_o + 4d_{pxo} - 2f_{xo})}{2}\cos 2\psi + \frac{\epsilon^2}{2}\left(2m_o(\log\frac{8}{\epsilon} - \frac{1}{2}) + 4f_{xo}(\log\frac{8}{\epsilon} + \frac{1}{2})\right) \quad (25)$$

$$\epsilon\cos\psi = 2\,\epsilon m_o\cos\psi - \frac{\epsilon^2(m_o + 4d_{pxo} - 2f_{xo})}{2}\sin 2\psi. \quad (26)$$

At $O(\epsilon)$, we get the strength of the rotlet as $m_o = \frac{1}{2}$ which is the central result of [10].

Equations (25) and (26) also justify the use of only the rotlet, the Stokeslet and the potential dipole in the expansion since the boundary conditions can be satisfied using these singularities. The higher order terms from these singularities can be balanced by additional singularities like the r directional stokeslet, but we restrict the analysis here to $O(\epsilon^2)$.

Equations (25) and (26) can be solved in two situations which we now discuss.

2.1 Calculation of the velocity of a force free rotating torus

The velocity of a force free torus is obtained by substituting $f_{xo} = 0$ in equations (25) and (26). The strength of the dipole can be obtained from equation (26) as $d_{pxo} = -\frac{1}{8}$. Equation (25) indicates that the x velocity is given by

$$U_x = \frac{\epsilon^2}{2}\left(\log\frac{8}{\epsilon} - \frac{1}{2}\right). \quad (27)$$

This is the nondimensional translational velocity of a freely rotating torus. The dimensional velocity of a rotating torus with an angular velocity ω can therefore be given by

$$\tilde{U}_x = \frac{\omega b^2}{2a}\left(\log\frac{8a}{b} - \frac{1}{2}\right). \quad (28)$$

which is exactly identical to the well known expression for velocity due to an ideal vortex ring as predicted by the potential flow theory [17,18]. This is expected because formally a rotlet u_{rot} is also the expression for the velocity field of an ideal line vortex. However, despite the kinematic analogy between the twirling torus and an ideal vortex ring, the physics behind is quite different. The propagation of an ideal vortex ring does not require any external forces/torques and is governed by conservation of kinetic energy and momentum. In sharp contrast the low Reynolds-number flow is governed by the dissipation in the fluid, which is manifested as a local force and a local torque acting on the torus. The rotating torus at low Reynolds numbers has to constantly dissipate energy to maintain its rotation as opposed to the inertia dominated ideal vortex ring [17,18].

If we consider a rotating torus as a model of a self propelled organism [3], the translational velocity is proportional to the "internal velocity" ω and quadratic in the ratio (b/a) in agreement with the previous results for the models of swimming of microorganism [5,4].

2.2 Calculation of force on a non-translating torus

To calculate the velocity field due to a rotating torus, prevented from translating by an external force, consider equations (25) and (26). Here $m_o = \frac{1}{2}$ satisfies the $O(\epsilon)$ equation. At $O(\epsilon^2)$, the quantities dependent on the angular parts can be balanced appropriately by $d_{pxo} = \frac{2f_{xo} - m_o}{4}$. The Stokeslet strength f_{xo} can be calculated by equating the translational velocity to zero, and the strength of the Stokeslet can now be easily determined as

$$f_x = -\frac{\epsilon^2}{4}\left[\frac{\ln(8/\epsilon) - 1/2}{\ln(8/\epsilon) + 1/2}\right]. \quad (29)$$

The strength of the potential dipole is then given by

$$d_{pxo} = -\frac{1}{4}\frac{\log\frac{8}{\epsilon}}{\log\frac{8}{\epsilon} + \frac{1}{2}}. \quad (30)$$

The local stress tensor can be expressed as $\mathbf{T} = [(\sigma_{xx}, \sigma_{xr}), (\sigma_{rx}, \sigma_{rr})]$, where different elements of the stress tensor have following definitions:

$$\sigma_{xx} = -p + 2\frac{du_x}{dx} \tag{31}$$

$$\sigma_{xr} = \sigma_{rx} = \frac{du_x}{dr} + \frac{du_r}{dx} \tag{32}$$

$$\sigma_{rr} = -p + 2\frac{du_r}{dr}. \tag{33}$$

The traction vector (force per unit area) is $\mathbf{t} = \mathbf{Tn}$, and its value in the x direction is given by $\mathbf{e_x Tn}$, where $\mathbf{n}$ is the unit normal given by $(\cos\psi, \sin\psi)$. The net force on the torus is then calculated by integrating the traction over the area of the torus given by $\int d\psi(1 + \epsilon\sin\psi)2\pi\,\epsilon$. Thus the net x directional non-dimensional force is given by

$$F_x = \int_0^{2\pi} d\psi(1 + \epsilon\sin\psi)2\pi\epsilon t_x = 4\pi^2\epsilon^2\frac{\ln(8/\epsilon) - 1/2}{\ln(8/\epsilon) + 1/2} \tag{34}$$

and the dimensional force by

$$\tilde{F_x} = 4\pi^2\mu b^2\frac{\ln(8/\epsilon) - 1/2}{\ln(8/\epsilon) + 1/2}. \tag{35}$$

The main contribution to the force therefore comes from the Stokeslet and has two parts: the skin drag due to viscous stresses and the form drag due to pressure variation around the torus. Unlike the case of a sphere where the form drag is half the skin drag, it is found that for the torus the two are of the same magnitude and given by $2\pi^2\,\epsilon^2\frac{\ln(8/\epsilon)-1/2}{\ln(8/\epsilon)+1/2}$.

The net torque on the torus about the centerline is given by the moment of the tangential force which is given by $\mathbf{tTn}$ about the center (lever arm ϵ)

$$N_c = \int d\psi(1 + \epsilon\sin\psi)2\pi\,\epsilon(\mathbf{tTn}\,\epsilon) = 8\pi^2\,\epsilon^2\left(1 - \epsilon^2\left(\frac{5}{16} + \frac{1}{8}\frac{\ln(8/\epsilon) - 1/2}{\ln(8/\epsilon) + 1/2}\right)\right)\mathbf{e}_\theta \tag{36}$$

and hence the net torque integrates out to zero. The dimensional, **locally felt**, torque is given by

$$\tilde{N_c} = 8\pi^2\mu b^2 a\left(1 - \epsilon^2\left(\frac{5}{16} + \frac{1}{8}\frac{\ln(8/\epsilon) - 1/2}{\ln(8/\epsilon) + 1/2}\right)\right)\mathbf{e}_\theta \tag{37}$$

One should note though, that, to maintain the local torque some form of internal driving mechanism of the torus is needed, which is possibly provided by the metabolic activity of the swimmer,or rectification of thermal motion as in [8].

3 The boundary integral method (BIM)

The results in the slender limit are practically useful, especially, in the case of polymer rings and miniplasmids. It would, however, be interesting to extend the results to the case in which the torus thickness is of the same order as the internal radius. For the motion of such a non-slender torus it is necessary to revert to some kind of numerical method. Here we use the boundary integral method which is a singularity method and is best suited to solve Stokes equations. The drag calculation (resistance problem) involves solving integral equation of the first kind, which are known to generate ill conditioned matrices [15], although converged non-oscillatory solutions are reported in certain specific cases [19]. For force calculation in the torus, we do get well behaved converged solutions which are in good agreement with the analytical solution in the slender torus limit. The calculations are then extended to the non-slender limit. In fact, the analytical expressions reported in Section 2 are multipole expansions of the complete integral equation, for force distribution, which can be solved numerically using the boundary integral method [16]. Note that multipole expansions are different moments of the Stokeslet about the centerline of the torus [16].

The representation of the velocity by the boundary integral equation can be written as

$$u_i(\mathbf{x}_0) = -\frac{1}{4\pi\mu}\int dS(\mathbf{x})G_{ij}(\mathbf{x},\mathbf{x}_0)f_j(\mathbf{x}) + \frac{1}{4\pi}\int dS(\mathbf{x})u_j(\mathbf{x})T_{ijk}(\mathbf{x},\mathbf{x}_0)n_k(\mathbf{x}) \tag{38}$$

where $G_{ij}(\mathbf{x},\mathbf{x}_0) = \left(\frac{\delta_{ij}}{r} + \frac{\mathbf{x}_i\mathbf{x}_j}{r^3}\right)$and $T_{ijk}(\mathbf{x},\mathbf{x}_0) = \frac{-6\,x_i x_j x_k}{r^5}$ where $r = |\mathbf{x} - \mathbf{x}_0|$, S(x) is the surface area of the body over which integration is carried out and n_k is the local unit outward normal to the surface. However, the second term in this equation can be modified [15] to avoid singular kernels and equation (38) can be solved numerically if suitably modified (Eq. (73), discussed in Appendix C). We make use of the axisymmetry in the problem, akin to the analytical solution discussed in the earlier section. The Greens functions are modified after integration in the azimuthal direction and are provided in several references [15,16]. These are expressed in terms of elliptic integrals of the first and second kind. In the above equation $u_i(\mathbf{x})$ is given by $(U_x + (1-r), x)$. The unknowns $f_j(x)$ are then solved for by numerically evaluating the integrals by discretizing the arc length into numerous elements and interpolating using cubic splines. The additional unknown U_x is obtained by imposing the no-force in the x direction condition which is $\int dS(\mathbf{x})f_x(\mathbf{x}) = 0$. The Greens function exhibit $-\log r$ singularity as $r \to 0$ that is $\mathbf{x} \to \mathbf{x}_0$. The singularity is handled in the usual way [15] by subtracting the singular part from the Greens functions and carefully integrating it analytically. The force, arc length and all other variables are also expressed as cubic splines. The condition of no net x directional force (force free torus) is enforced to get the unknown longitudinal translational velocity. The comparison of the asymptotic and numerical solutions are discussed in the following section. In all the simulations reported in this work, we have used 80 elements for discretization. The simulations were repeated

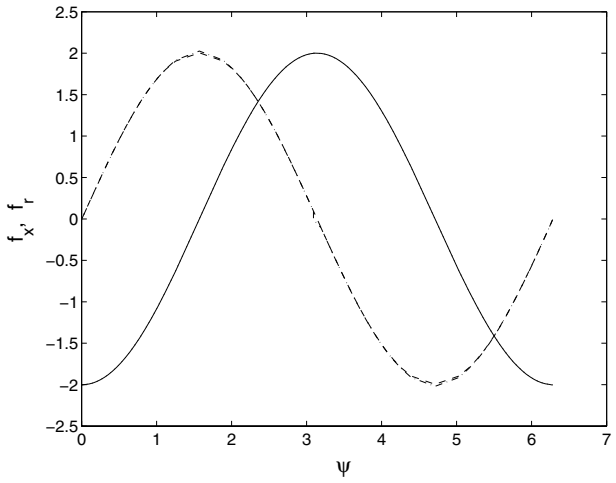

Fig. 4. Comparison of the analytical and numerical x and r directional forces for a slender ($\epsilon = 0.025$) torus (—, F_x(Num), $\cdots$, F_x(Anal), — · —·, F_r(Num), ----, F_r(Anal)). Note that the analytical and numerical results are identical and almost indistinguishable.

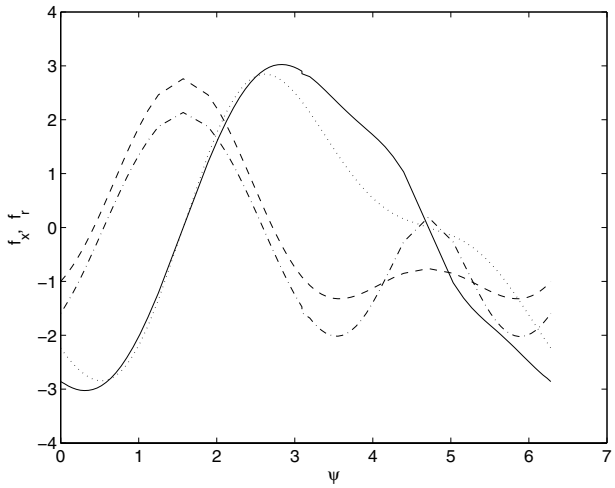

Fig. 5. Comparison of the analytical and numerical x and r directional forces for a non-slender ($\epsilon = 0.5$) torus (—, F_x(Num), $\cdots$, F_x(Anal), — · —·, F_r(Num), ----, F_r(Anal))

with 160 elements and no significant difference was obtained up to the third decimal place.

4 Comparison of analytical and numerical results

The results derived for a freely rotating torus require a force and torque free motion. However, locally at each point on the torus, there is a finite force and torque acting and analytical expressions can be easily obtained as $\mathbf{t}\cdot\mathbf{T}\cdot\mathbf{n}$, where $\mathbf{T}$ is given by equations described in section 2.2.

$$f_x = \frac{(16 + 6\epsilon^2 - 3\epsilon^2(\cos 2\psi + \log 64 - 2\log\epsilon))\sin\psi}{8} - 2\epsilon\cos 2\psi \tag{39}$$

$$f_r = -\frac{\cos\psi(16 - 6\ \epsilon^2 +\ \epsilon(-3\ \epsilon(\cos 2\psi - \log 64 + 2\log\ \epsilon)}{8} - 4\sin\psi\cos\psi. \tag{40}$$

Note that both the forces when integrated over the surface of the torus equate to zero, indicating a globally force free, torque free torus. Figure 4 compares the numerical solution with the analytical expressions for the forces (Eqs. (39, 40)) and shows a good agreement in the slender torus limit. At higher values of ϵ, a deviation between the numerical and analytical results is clearly seen (Fig. 5).

The main analytical results from the calculations is equation (27) which gives the translational propulsion velocity as a function of the angular velocity and the aspect ratio of the torus.

Figure 6 shows the comparison of the analytical (Eq. (27)) and numerical results for the translational velocities. Interestingly, the analytical expressions are valid

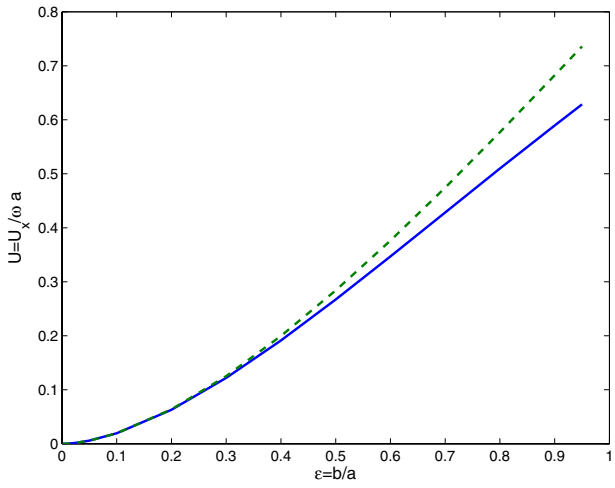

Fig. 6. Comparison of the numerical (—) and analytical (----) translational velocity

for slenderness ratio as high as 0.5. This can be attributed to the $O(\epsilon^2)$ analysis carried out in the present work. For a really "fat" torus, the translational velocities are lower than those predicted by the analytical slender limit results. A "fatter" torus seems to be slower than that predicted analytically, which could be due to the hydrodynamic interaction of the flow fields of various sections of the moving torus.

5 Mobility and resistance matrices

Mobility and resistance matrices are commonly used in describing the collective hydrodynamics of a group of particles, where the forces and the torques are related to the translational and rotational velocities of the particles. The resistance or the mobility matrices are dense, although symmetric. However, for single particles, the matrices are

often diagonal, indicating that the forces typically cause translation and torques cause rotation. A torus is one of the few bodies with a regular geometry in which a resistance matrix can be written even for a single particle (torus) due to the coupling of the torques and forces. Here we derive a resistance matrix (M_{kl}) in terms of dimensional quantities, relating the angular velocity ω_c (about the circular axis) and velocity u_x (in the x direction) with the corresponding external torque $\tilde{N}_c$ and force $\tilde{F}_x$, so that

$$\begin{pmatrix} F_x \\ N_c \end{pmatrix} = 4\pi^2\mu \begin{pmatrix} M_{11} & M_{12} \\ M_{21} & M_{22} \end{pmatrix} \begin{pmatrix} u_x \\ \omega_c \end{pmatrix}.$$

Combining the previous expressions obtained for F_x and N_c (Eqs. (34) and (37)), together with the results for a translating torus (Appendix B, [9]) for the drag on a rigid slender torus, we obtain the entries for the mobility matrix $\mathbf{M}$ at the leading order as:

$$\mathbf{M} = \begin{pmatrix} M_{11} & M_{12} \\ M_{21} & M_{22} \end{pmatrix}.$$

Such that

$$\begin{aligned} M_{11} &= 2a(\log 8/\epsilon + 1/2)^{-1} \\ M_{12} &= M_{21} = b^2(\log 8/\epsilon - 1/2)(\log 8/\epsilon + 1/2)^{-1} \\ M_{22} &= 2b^2a. \end{aligned} \tag{41}$$

Note that the symmetry of the resistance matrix is a general feature of swimmers in Stokes flow and provides a good check for the consistency of the involved calculations.

The numerical results for propulsion velocity in the paper are in agreement with [14].

6 Motion of a torus along a cylindrical rod

It is interesting to study the motion of a torus along a cylindrical rod, since the direction of motion can possibly reverse as the diameter of the cylindrical rod is made larger [7]. Such a setup has been suggested [8] in the case of a nanomachine, essentially a DNA mini-plasmid, suitably selected, so that it can be converted into a nanoswimmer. It was argued that although the mini-plasmid could, under certain circumstances, self-propel, its effect can be nullified by the substantial out of plane rotational diffusion prevalent in these machines owing to their small sizes [11]. It was therefore proposed to thread a DNA through the center of the DNA miniplasmid thereby allowing only unidirectional motion. This situation was first addressed by Taylor [7], albeit qualitatively and the calculations were not provided. In another study Cox and O'Neil separately [12,13] obtained analytical solutions for the case of a slender torus moving inside a tube, in two different parameter regimes: non-lubrication and lubrication. They obtained the force on the torus when it is sliding both inside as well as outside of an infinitely long cylinder. However, there are no calculations to date which address the motion of a force free, rotating torus along a circular cylinder, and its propulsion velocity, which is exactly

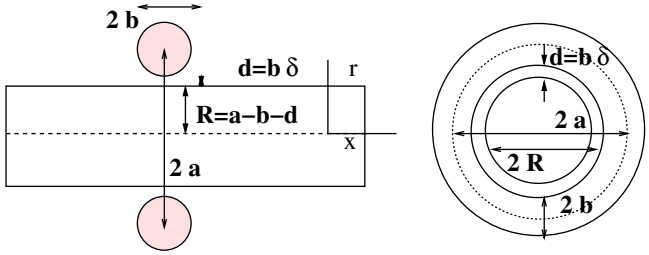

Fig. 7. Schematics of a torus moving along a rod.

the proposed mechanism by [8] of a DNA mini-plasmid on a track (Fig. 1b). The system can be best described in cylindrical coordinates. We work here with dimensional quantities and follow the same notation as that of [12]. Consider a torus (Fig. 7) translating in the x direction with velocity U and rotating about its centerline with angular velocities ω. The torus has smaller and larger radius, b and a, and moves along an infinitely long inner cylinder of radius R. We introduce two small parameters here, ϵ and δ, such that the distance between the torus surface and the cylinder $d = a - b - R = \delta b$ and $b = \epsilon a$, which correspond to lubrication limit of a slender torus. In addition, we describe the parameter $\beta = R/a = 1 - \epsilon - \epsilon\delta$ in conjunction with the notations used in [12] and [13] such that $\beta > 1$ indicates a torus translating inside a cylinder and $\beta < 1$ denotes a torus moving outside an infinitely long cylinder. For $\beta < 1$, $\beta \to 0$ ($R \ll a$)indicates limit of weak wall effect and $\beta \to 1$ ($R \approx a$) indicates presence of strong wall effect. Suitable non-dimensional variables described here are relevant only to this section. The equations of motion at low Reynolds number (taking advantage of the azimuthal symmetry) can be written as:

$$\frac{1}{r}\frac{\partial(ru_r)}{\partial r} + \frac{\partial u_x}{\partial x} = 0 \tag{42}$$

$$-\frac{\partial p}{\partial r} + \mu\left[\frac{\partial^2 u_r}{\partial r^2} + \frac{1}{r}\frac{\partial u_r}{\partial r} - \frac{u_r}{r^2} + \frac{\partial^2 u_r}{\partial x^2}\right] = 0 \tag{43}$$

$$-\frac{\partial p}{\partial x} + \mu\left[\frac{\partial^2 u_x}{\partial r^2} + \frac{1}{r}\frac{\partial u_x}{\partial r} + \frac{\partial^2 u_x}{\partial x^2}\right] = 0. \tag{44}$$

The boundary conditions are the following: at $r = R = a - b - d$, the velocity $u_x, u_r = 0$, and on the surface of the torus $u_x = \omega(a - r) + U, u_r = \omega x$.

One of the motivations for earlier works on this configuration [12,13] of a torus sedimenting inside a cylinder was to explain the experimental results of a translating torus [20]. The geometry was selected because the experimental results showed deviation from the predictions of a sedimenting torus in an infinite medium and the discrepancy was attributed to the presence of the walls of the cylindrical vessel in which the experiments were carried out. In these studies, analysis was performed using singularity method for two different regimes, $\beta \to 1$ and $\beta \to 0$, which correspond to strong and weak wall effects respectively. The work was also extended to the case of a torus sedimenting on the outside and along the axis of an infinitely long cylinder ($\beta < 1$) [12], which is also the

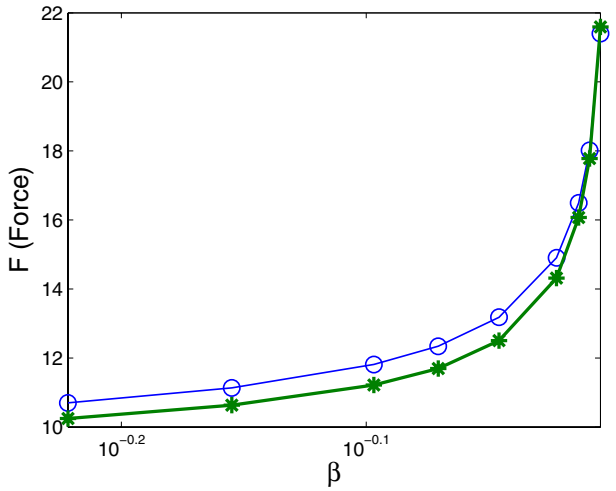

Fig. 8. Comparison of the variation of the total force (F) with $\beta = R/a$ of [12] ($\circ$) and the present BIM study (*) for a sedimenting torus $U = 1.0, a = 1.0, \mu = 1.0,\ \epsilon = 0.0005$.

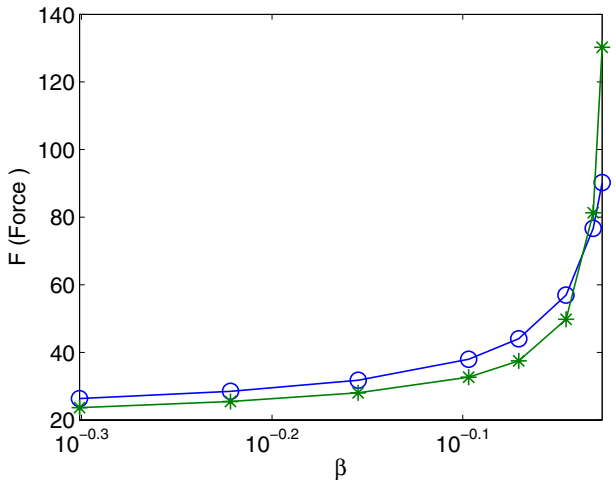

Fig. 9. Comparison of the variation of the total force (F) with $\beta = R/a$ of [12] ($\circ$) and the present BIM study (*) for a sedimenting torus $U = 1.0, a = 1.0, \mu = 1.0,\ \epsilon = 0.05$.

case in the present study, and again, both $\beta \to 1$ and $\beta \to 0$ regimes were considered. The analytical expression for the total force acting on the torus in the $\beta \to 1$ is given by [12],

$$F = \frac{8\pi^2 a\mu U}{\ln \frac{2(a-R)}{b}}, \tag{45}$$

for the parameter regime $\epsilon < \delta < 1$. We use the boundary integral method, described in the earlier section, to calculate the drag force on the torus sedimenting along a cylinder. The only difference in this case is that the integration is performed over both the torus and the cylinder areas, axi-symmetry being still valid. The results of [12] are verified first, and comparisons made with the analytical expression (Eq. (45)). Typically, the infinitely long cylinder was kept 80 times the larger torus diameter ($a = 1$) and 160 elements were equally distributed over the cylinder and rod. The results were verified by doubling the length of the cylinder and the number of elements.

Figure 8 shows the comparison of the results obtained from the present BIM study with the expression given by [12] (Eq. (45)). For $\epsilon = 0.0005$, the results show a very good agreement, however, for $\epsilon = 0.05$ (Fig. 9, it is found that the deviation is large especially for $\beta \to 1$. This is expected since the results of [12] are valid in the limit $\epsilon < \delta < 1$, whereas for a given ϵ, $\delta \to 0$ as $\beta \to 1$, the assumption, $\epsilon < \delta$ in [12] is violated. Note that $\beta = 1 - \epsilon(1-\delta)$. In the present work, we are interested in the regime $\delta < \epsilon < 1$ for a torus rotating about its centerline and translating along the cylinder axis. Thus, the limit considered is one in which, the slender torus moves along the cylinder at gap widths δ much smaller than the smaller diameter of the torus.

At the leading order a torus rotating about its centerline with a cylinder passing through its center is identical to a rotating cylinder near an infinite wall in the lubrication limit. Therefore, a naive lubrication theory analysis of this problem indicates that the torque on a translating torus along a cylinder or the force on a rotating torus is zero. This is identical to the result obtained by [21] for a rotating and translating cylinder near a wall exerting zero force and torque respectively.

The numerical results however show that the force on a rotating or translating torus about a cylinder is non-zero [12,13]. The reason for this can be attributed to the fact that unlike the case of a cylinder, the torus has a finite length $l = 2\pi a$ with a curvature of the order of $1/a$ and has an internal degree of freedom.

We now extend the analysis to the case of a force free torus, rotating at a constant angular velocity ω and moving along the cylinder, using the boundary element method. To solve for the force free torus, we adopt a strategy similar to that for a single self-propelled torus. The integral equation is solved for the unknown stokeslet strength f_i with an additional constraint that the net force vanishes $\int dS(x) f_i(x) = 0$. This extra equation allows the calculation of the unknown propulsion velocity U_s. To describe the results in a compact way, we nondimensionalise the lengths as earlier with the outer torus diameter, a and the velocities are with $a\omega$. We report the force free translational (propulsion) velocity scaled by the non dimensional single torus (in an infinite fluid) velocity $U_s = \epsilon^2/(\log(8/\epsilon) - 1/2)$ so that $U^* = U/U_s$. Figure 10 indicates that the torus undergoes reversal of direction as the thickness of the inner cylinder increases. At small thicknesses of the cylinder ($\beta \to 0$), the torus is propelled by the theory discussed earlier for a single rotating torus indicated by $U^* = 1$. However even for very small thicknesses of the cylinder, substantial deviations are observed from that of a freely rotating torus which is typical of Stokes flow. As the thickness of the inner cylinder is increased the translational motion reverses and the torus now starts moving in the opposite direction ($\beta \to 1$). This is the rolling motion observed for force free rotating objects near a solid wall (Fig. 12). To get the correct scaling of rotation in the lubrication limit, we carried out

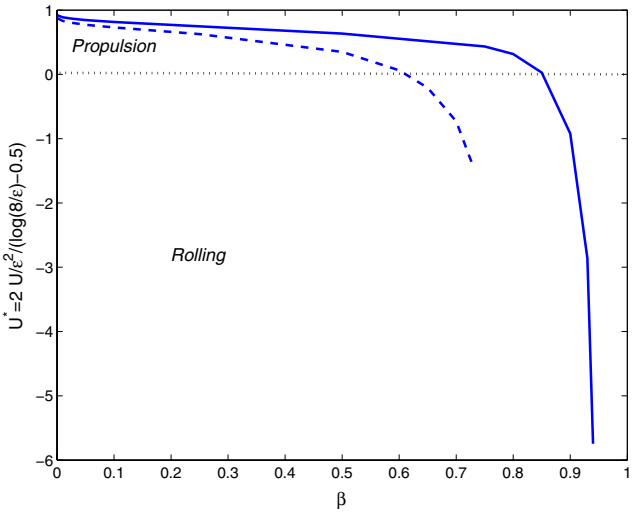

Fig. 10. Variation of the scaled translation velocity with the the scaled cylinder thickness for slenderness ratio — $\epsilon = 0.05$, ---- $\epsilon = 0.25$.

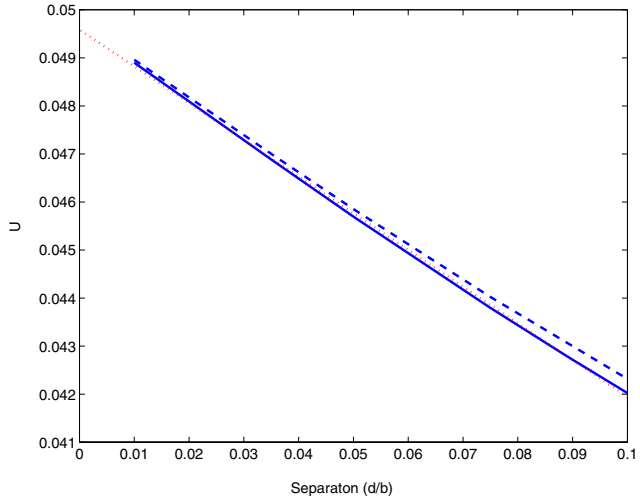

Fig. 11. Comparison of dimensional translational (Rolling) velocity in the lubrication limit for two different inner diameters of a torus ($b = 0.05$, —$a = 1$, ----$a = 2$, ····· Best fit $U = 0.05\ b(1–3/2\ d/b)$).

simulations in low gap limit in dimensional quantities. Figure 11 shows the variation of the dimensional translational velocity as a function of the gap distance for two different tori diameter $a = 1$ and $a = 2$. The velocity is seen to vary as

$$U = b\omega\left(1 - \frac{3}{2}\frac{d}{b}\right) \tag{46}$$

where $d = b\delta$ is the dimensional separation. The result indicates that the rolling velocity is independent of the torus diameter. This can be compared with the result for the rolling of a force free sphere of radius a for which the translational velocity goes as $U = a\omega/4$ [22] and the deviation from $a\omega$ by a factor of 4 is described as the slip, a result discussed in details in the literature. The force free cylinder on the other hand does not show any translation [21]. The numerical results for the torus show a clear scaling of $U \sim b\omega$ for the translational velocity in the limit of separation $d \to 0$.

7 Conclusion

The paper presents analytical and numerical calculations for a rotating torus. The analytical results are valid up to $O(\epsilon^2)$ in the slenderness ratio. The calculations reveal that a rotating torus can translate. The reason for this can be attributed to the presence of non-zero non-diagonal terms in the reduced mobility and resistance matrices. The expression for the translational velocity is identical to that of translating smoke rings in inviscid flow. Such a translating torus is force free and torque free. The force and torque required to prevent the translation of a rotating torus is also calculated. The results of slender torus are extended numerically to finite aspect ratio using the boundary integral method. It is found that the analytical expression provided is correct to a slenderness ratio as high as 0.2 which is attributed to the $O(\epsilon^2)$ analysis. The

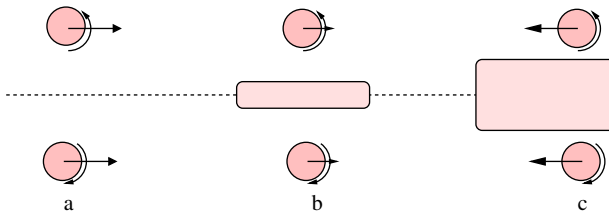

Fig. 12. Schematic of transition from propulsion to rolling regime, (a) propulsion of a free torus, (b) propulsion of a torus moving along a cylinder, (c) rolling of a torus along a cylinder.

local forces and torques are also calculated. Finally the mobility matrix for the rotating-translating torus is provided. The results would be of immense use in calculating the friction and writing the correct Langevin equations for DNA mini-plasmids of different slenderness ratio which is the subject of our future publication. The results for the motion of a slender torus along a cylinder show that the torus can undergo reversal of translational motion from a propulsion type to rolling when the internal diameter of the cylinder is changed. Interestingly, the translational velocity is found to be independent of the size of the torus in the lubrication limit.

We thank one of the referees for bringing to our notice a similar work [14]. The authors in that paper have addressed propulsion of a Purcell's swimmer using toroidal coordinates. The final results are obtained in a numerical fashion and are in agreement with the results of our present work. The emphasis in the aforesaid work though is on the efficiency of such a swimmer and comparison of a toroidal swimmer with a similar object made from a collection of rotating spheres.

Appendix A: Elliptic Integrals

The complete elliptic integrals are defined as [23]:

$$F(k) = \int_0^{\pi/2} \frac{d\theta}{\sqrt{1-k^2\sin^2\theta}} \tag{47}$$

$$E(k) = \int_0^{\pi/2} d\theta \sqrt{1-k^2\sin^2\theta}. \tag{48}$$

The elliptic integrals have the following asymptotic expansion around $k = 1$,

$$F(k) = \frac{1}{2}\ln\left(\frac{16}{1-k^2}\right) \tag{49}$$

$$E(k) = 1 + \frac{1-k^2}{2}\left(\ln\frac{16}{1-k^2} - \frac{1}{2}\right) \tag{50}$$

and around $k = 0$, the asymptotic expression reads

$$F(k) = \frac{\pi}{2} + \frac{\pi}{8}\,k^2 + \frac{9\pi k^4}{128} \tag{51}$$

$$E(k) = \frac{\pi}{2} - \frac{\pi}{8}\,k^2 - \frac{3\pi k^4}{128}. \tag{52}$$

$$I_1 = \int_0^{2\pi} \frac{d\theta}{\sqrt{1-k\cos^2\theta/2}} = 4F(k) \tag{53}$$

$$I_2 = \int_0^{2\pi} \frac{\cos\theta}{\sqrt{1-k\cos^2\theta/2}} d\theta = \frac{4}{k}\left((2-k)F(k) - 2E(k)\right)$$

$$I_3 = \int_0^{2\pi} \frac{d\theta}{\sqrt[3]{1-k\cos^2\theta/2}} = \frac{4}{1-k}E(k)$$

$$I_4 = \int_0^{2\pi} \frac{\cos\theta}{\sqrt[3]{1-k\cos^2\theta/2}} d\theta = \frac{4}{k}\left(\frac{2-k}{1-k}E(k) - 2F(k)\right)$$

$$I_5 = \int_0^{2\pi} \frac{\cos^2\theta}{\sqrt[3]{1-k\cos^2\theta/2}} d\theta = \frac{4}{k^2}\left(\frac{k^2-8k+8}{1-k}E(k) - 4(2-k)F(k)\right)$$

$$I_6 = \int_0^{2\pi} \frac{d\theta}{\sqrt[5]{1-k\cos^2\theta/2}} = \frac{4}{3(1-k)}\left(\frac{2}{1-k}(2-k)E(k) - F(k)\right)$$

$$I_7 = \int_0^{2\pi} \frac{\cos\theta}{\sqrt[5]{1-k\cos^2\theta/2}} d\theta = \frac{4}{3k(1-k)}\left(\frac{2}{1-k}(1-k+k^2)E(k) - (2-k)F(k)\right)$$

$$I_8 = \int_0^{2\pi} \frac{\cos^2\theta}{\sqrt[5]{1-k\cos^2\theta/2}} d\theta = \frac{4}{3k^2(1-k)} \times \left((8-8k-k^2)F(k) - \frac{2(2-k)(2-2k-k^2)}{1-k}E(k)\right)$$

$$I_9 = \int_0^{2\pi} \frac{\cos^3\theta}{\sqrt[5]{1-k\cos^2\theta/2}} d\theta = \frac{4}{3k^3(1-k)}\left(\frac{2}{2-k}(k^4+k^3-33k^2+64k-32)E(k)\right) + \frac{4}{3k^3(1-k)}\left(-(2-k)(k^2+32k-32)F(k)\right). \tag{54}$$

Appendix B: Analytical solution for a translating, non-rotating torus

The force and torque acting on a translating torus was calculated by Johnson [9], apart from several other results. We rederive these equations using the method outlined here and arrive at the same results. The method described is general enough and can be easily extended to the calculation of hydrodynamic interaction between two tori which is a subject of our future publication.

Constructing velocity profiles for a translating torus

For a torus translating in the x direction with velocity U, we scale the lengths by a, the velocity with U, time by a/U, the stresses and the pressure by $\mu a/U$. The θ component of the velocity goes to zero by symmetry. The velocities are easily expressed in terms of complete elliptic integrals with a ring of Stokeslet, dipoles and rotlets as

$$u_x = \frac{m}{C^3}(I_3 - rI_4) + d_{px}\left(\frac{I_3}{C^3} - 3x^2\frac{I_6}{C^5}\right) + f_x\left(\frac{I_1}{C} + x^2\frac{I_3}{C^3}\right) \tag{55}$$

$$u_r = \frac{mxI_4}{C^3} - \frac{3d_{px}x}{C^5}(rI_6 - aI_7) + \frac{xf_x}{C^3}(rI_3 - I_4)$$

$$p = \frac{2f_x x I_3}{C^3}. \tag{56}$$

where p is the pressure due to the Stokeslet.

The boundary conditions for the problem are $\tilde{u}_x^s = U$ and $\tilde{u}_r^s = 0$ at the surface of the torus. The non-dimensional boundary conditions become $u_x^s = 1$ and $u_r^s = 0$. We consider here the case of a slender torus (the ratio of the two radii of the torus, $\epsilon = b/a$ is small), and the surface can be locally parameterized by an angle ψ, such that $x = \cos\psi$ and $r = 1 + \epsilon\sin\psi$. The boundary conditions demand a scaling, $m = m_0\epsilon^2$, $d_{px} = \epsilon^2 d_{po}$, and $d_{po} = f_x/2$, with $f_x = O(1)$. The boundary conditions are given by,

$$u_i^s = u_i(S) \tag{57}$$

$$\int_0^{2\pi} d\theta (x \times u_i^s) = \int_0^{2\pi} d\theta (x \times u_i(S)), \tag{58}$$

where u_i^s is the velocity on the surface of a torus Ue_x. Integrating equation (57) leads to,

$$U = f_o \left(1 + 2\log\frac{8}{\epsilon}\right), \tag{59}$$

such that,

$$f_o = \frac{U}{(1 + 2\log\frac{8}{\epsilon})}. \tag{60}$$

Similarly, the strength of the rotlet is obtained by integrating equation (58) over the surface of the torus. The method is similar to deriving Faxen's second law for a sphere [24] and requiring that the velocity on the surface is $u_i^s = Ue_x$ gives,

$$m_0 = -f_0\frac{\log\frac{8}{\epsilon} - 1}{2}. \tag{61}$$

Calculation of force and torque on a translating torus

The stress tensor is expressed as $\mathbf{T} = [(\sigma_{xx}, \sigma_{xr}), (\sigma_{rx}, \sigma_{rr})]$, where the different elements of the stress tensor have following definitions:

$$\sigma_{xx} = -p + 2\frac{du_x}{dx} \tag{62}$$

$$\sigma_{xr} = \sigma_{rx} = \left(\frac{du_x}{dr} + \frac{du_r}{dx}\right) \tag{63}$$

$$\sigma_{rr} = -p + 2\frac{du_r}{dr}. \tag{64}$$

The traction vector (force per unit area) is $\mathbf{t} = \mathbf{Tn}$, and the traction in the x direction is given by $\mathbf{e_x} \cdot \mathbf{Tn}$, where $\mathbf{n}$ is the unit normal given by $(\cos\psi, \sin\psi)$. The net force on the torus is then calculated by integrating the traction over the area of the torus given by $\int d\psi(1 + \epsilon\sin\psi)2\pi\ \epsilon$. Thus the non-dimensional net x directional force per unit center line length (2π) is given by

$$F_x = \int_0^{2\pi} d\psi(1 + \epsilon\sin\psi)2\pi\epsilon t_x = -\frac{16\pi^2}{1 + 2\log 8/\epsilon} \tag{65}$$

and the dimensional force is given by

$$\tilde{F_x} = -\frac{8\pi^2 a\mu U}{\log\frac{8}{\epsilon} + \frac{1}{2}}. \tag{66}$$

The net torque on the torus about the centerline is given by the moment of the tangential force which is given by $\mathbf{tTn}$ about the center (lever arm ϵ)

$$N_c = \int d\psi\frac{(1 + \epsilon\sin\psi)2\pi\epsilon}{2\pi}(\mathbf{tTn}\epsilon) = 4\pi^2\epsilon^2(f_0 - 4m_0)$$
$$= 4\pi^2\ \epsilon^2\frac{\log 8/\epsilon - 1/2}{\log 8/\epsilon + 1/2} \tag{67}$$

and the total dimensional torque is given by

$$\tilde{N_c} = 4\pi^2\mu b^2 U\frac{\log 8/\epsilon - 1/2}{\log 8/\ \epsilon + 1/2}. \tag{68}$$

Expressions (66) and (68) are the central results of [9].

Appendix C: Derivation of boundary integral equation

The basic equation for velocity at a point in flow over a particle, when the point lies outside the particle is given by

$$u_i(\mathbf{x}_0) = -\frac{1}{8\pi\mu}\int dS(\mathbf{x})G_{ij}(\mathbf{x}, \mathbf{x}_0)f_j(\mathbf{x}) + \frac{1}{8\pi}\int dS(\mathbf{x})u_j(\mathbf{x})T_{ijk}(\mathbf{x},\mathbf{x}_0)n_k(\mathbf{x}). \tag{69}$$

The first integral is called as single layer potential, whereas the second is called the double layer potential. When the singular point is moved on to the surface, the equation is modified as

$$u_i(\mathbf{x}_0) = -\frac{1}{4\pi\mu}\int dS(\mathbf{x})G_{ij}(\mathbf{x}, \mathbf{x}_0)f_j(\mathbf{x}) + \frac{1}{4\pi}\int dS(\mathbf{x})u_j(\mathbf{x})T_{ijk}(\mathbf{x},\mathbf{x}_0)n_k(\mathbf{x}). \tag{70}$$

The singularity in the double layer potential can be eliminated by re-writing the equation as

$$u_i(\mathbf{x}_0) = -\frac{1}{4\pi\mu}\int dS(\mathbf{x})G_{ij}(\mathbf{x}, \mathbf{x}_0)f_j(\mathbf{x}) + \frac{1}{4\pi}\int dS(\mathbf{x})(u_j(\mathbf{x}) - u_j(\mathbf{x_0}))T_{ijk}(\mathbf{x},\mathbf{x}_0)n_k(\mathbf{x}) + u_j(\mathbf{x_0})\frac{1}{4\pi}\int dS(\mathbf{x})T_{ijk}(\mathbf{x},\mathbf{x}_0)n_k(\mathbf{x}). \tag{71}$$

Using the property of double layer potential,

$$\int dS(\mathbf{x})T_{ijk}\mathbf{x},\mathbf{x}_0)n_k(\mathbf{x}) = -4\pi\delta_{ij} \tag{72}$$

the governing equation can be re-written as

$$u_i(\mathbf{x}_0) = -\frac{1}{8\pi\mu}\int dS(\mathbf{x})G_{ij}(\mathbf{x}, \mathbf{x}_0)f_j(\mathbf{x}) + \frac{1}{8\pi}\int dS(\mathbf{x})(u_j(\mathbf{x}) - u_j(\mathbf{x_0}))T_{ijk}(\mathbf{x},\mathbf{x}_0)n_k(\mathbf{x}). \tag{73}$$

In the present work, it was found that the contribution of the second integral increases as the slenderness ratio ϵ increases. This is understandable as the assumption of rigid body approximation becomes more invalid with ϵ. However, the absolute contribution of the second integral was found to be minimal and results were affected by around 1% (if the second integral was neglected) even in the case of a torus of thickness $\epsilon = 0.8$. The change was less than 0.1% for slender tori ($\epsilon < 0.05$)

References

1. G.I. Taylor, Proc. R. Soc. London, Ser. A. **209**, 447 (1951)
2. M. Lighthill, Commun. Pure Appl. Math. **5**, 109 (1952)
3. E.M. Purcell, Amer. J. Phys. **45**, 3 (1977)
4. J. Avron, O. Gat, O. Kenneth, Phys. Rev. Lett. **93**, 186001 (2004)

5. N. Ali, R. Golestanian, J. Phys. Condens. Matter **17**, S1203 (2005)
6. R. Dreyfus, J. Baudry, M. Roper, M. Fermigier, H. Stone, J. Bibette, Nature **6**, 862 (2005)
7. G. Taylor, Proc. R. Soc. London, Ser. A **211**, 225 (1952)
8. I. Kulic, R. Thaokar, H. Schiessel, Europhys. Lett. **72**, 527 (2005)
9. R.E. Johnson, T.Y. Wu, J. Fluid Mech. **95**, 263 (1979)
10. A.T. Chwang, W.S. Hwang, Phys. Fluids **8**, 1309 (1990)
11. I.M. Kulic, R. Thaokar, H. Schiessel, J. Phys.: Condens. Matter **17**, S3965 (2005)
12. R.G. Cox, Chem. Engng. Comm. **148**, 563 (1996)
13. M.E. O'Neil, Chem. Engng. Comm. **148**, 161 (1996)
14. A. Leshansky, O. Kenneth, `cond-mat/physics.flu-dyn (2007)`
15. C. Pozrikidis, *Boundary integral and singularity methods for linearized viscous flow* (Cambridge University Press, Cambridge, 1992)
16. S. Kim, S. Kariala, *Microhydrodynamics* (Butterworth-Heinemann, MA, USA, 1991)
17. H. Lamb, *Hydrodynamics*, 6th edition (Cambridge University Press, Cambridge, 1993)
18. E. Guyon, J. Hulin, L. Petit, C. Mitescu, *Physical hydrodynamics* (Oxford University Press, Oxford, 2001)
19. G.K. Youngren, A. Acrivos, J. Fluid Mech. **6**, 377 (1975)
20. A. Amarakoon, R. Hussey, B. Good, E. Grimsal, Phys. Fluids **25**, 1495 (1982)
21. D.J. Jeffery, Y. Onishi, Quarterly J. Mech. Appl. Math. **34**, 129 (1981)
22. A.J. Goldman, R.G. Cox, H. Brenner, Chem. Engng. Sci. **22**, 637 (1964)
23. M. Abramowitz, I. Stegun, *Handbook of mathematical functions* (Dover, New York, 1964)
24. W. Russel, D. Saville, W. Schowalter, *Colloidal dispersions* (Cambridge University Press, Cambridge, 1989)